A Novel Approach for Analyzing the Structure of DNA Modified by Benzo[a]pyrene Diol Epoxide at Single-Molecule Resolution

ARTICLE *in* CHEMICAL RESEARCH IN TOXICOLOGY · JUNE 2000

Impact Factor: 3.53 · DOI: 10.1021/tx9902035 · Source: PubMed

3 AUTHORS, INCLUDING:

Lia Pietrasanta
University of Buenos Aires
61 PUBLICATIONS **2,097** CITATIONS
SEE PROFILE

Bettye L Maddux
Oregon State University
55 PUBLICATIONS **3,203** CITATIONS
SEE PROFILE

A Novel Approach for Analyzing the Structure of DNA Modified by Benzo[*a*]pyrene Diol Epoxide at Single-Molecule Resolution

Lía I. Pietrasanta,[†,‡] Bettye L. Smith,*[,†,‡] and Michael C. MacLeod[§]

Department of Physics, University of California, Santa Barbara, California 93106, and Department of Carcinogenesis, University of Texas M. D. Anderson Cancer Center, Smithville, Texas 78957

Received December 13, 1999

Benzo[*a*]pyrene diol epoxide (BPDE) has been shown to bind specifically to the exocyclic amino group of deoxyguanosine in duplex DNA. Interestingly, this metabolite exhibits stereoselectivity in its tumorigenic and mutagenic effects. It is thought that local DNA conformation is altered at the site of the adduct, resulting in aberrant biological processes, and that in certain sequence contexts BPDE−DNA adducts induce bends in the DNA. In the work presented here, we compared DNA structural alterations of BPDE-modified DNA and unmodified DNA via tapping mode atomic force microscopy (AFM). DNA fragments 366 base pairs (bp) in length were generated by PCR from the duplicated multiple-cloning site of pBEND2 inserted into pGEM-3Zf(−), and either mock-modified or treated with BPDE to give modification levels between 1 and 5% of the nucleotides. Control or BPDE-modified DNA was adsorbed to mica and visualized in air by AFM. The contour lengths and end-to-end lengths of individual molecules were measured. The ratio of end-to-end distance to contour length was significantly smaller for modified DNA molecules than for the unmodified DNA preparation, although the frequency distributions of the contour lengths were similar for the two preparations. This suggests BPDE−DNA adducts cause significant bending of DNA molecules, confirming previous conclusions based on more indirect measurements. The average induced bend angle for BPDE−DNA adducts is estimated to be at least 30°.

Introduction

The ultimate carcinogen 7r,8t-dihydroxy-9,10t-oxy-7,8,9,10-tetrahydrobenzo[*a*]pyrene (BPDE)[1] binds covalently to the exocyclic amino moiety of dGua both in vivo and in vitro (*1*−*3*). This lesion, if not repaired, causes numerous biological effects, including polymerase blockage, transcription factor hijacking, mutation induction, and, finally, carcinogenesis (*4*−*8*). There is evidence that the severity of these functional effects is dependent on the stereochemistry of the lesion and the base sequence around the lesion (*7*−*11*). The specificity of mutation induction is also dependent on other poorly understood parameters of DNA conformation (*11*, *12*). This has led to suggestions that adduct conformation is an important determinant of the qualitative and quantitative nature of the functional sequellae of DNA adduct formation, and led to attempts to understand possible deformations of DNA structure caused by BPDE−DNA adducts. Using spectroscopic and electrophoretic analytical techniques, both randomly generated BPDE adducts and site-specific adducts have been examined (*13*−*17*). In general, the data from these experiments have been interpreted to suggest that BPDE−DNA adducts in at least some sequence contexts induce a bend or flexible "hinge" in the DNA. However, to our knowledge no direct evidence of BPDE-induced bending of large DNA molecules has been published. We therefore undertook an analysis of the effects on the overall conformation of DNA of randomly induced BPDE−DNA adducts, using atomic force microscopy to visualize individual DNA molecules with defined lengths.

Materials and Methods

DNA was prepared from a pGEM-3-Zf(−)-derived plasmid containing the duplicated multiple-cloning site of pBEND2 (pGB) (*18*). pGB was used either directly or as a template in a PCR with m13 forward and reverse primers to amplify a 366 bp sequence. The product was isolated from a 1% agarose gel by electroelution, and concentrated by ethanol precipitation. The isolated linear 366 bp fragment or whole circular plasmid, pGB DNA, was redissolved in 10 mM Tris-HCl (pH 7.5), and aliquots were allowed to react with 7r,8t-dihydroxy-9,10t-oxy-7,8,9,10-tetrahydrobenzo[*a*]pyrene (BPDE) for 60 min at 37 °C. The BPDE was previously dissolved in tetrahydrofuran (THF) and added to the DNA solution to give a final THF concentration of 20% (v/v). The solution was adjusted to 0.1 M NaCl, and hydrolysis products were removed by multiple extractions with ethyl acetate and ether, followed by ethanol precipitation and ether extraction of the precipitate (*5*). Alternatively, aliquots of the DNA were mock-modified with solvent only as a control. Parallel reactions were conducted with salmon DNA, and the level of modification attained with a given concentration of BPDE was determined spectrophotometrically (*5*).

* To whom correspondence should be addressed: Department of Physics, University of California, Santa Barbara, CA 93106. E-mail: bettye@physics.ucsb.edu.

† University of California.

‡ These authors contributed equally to this work.

§ University of Texas M. D. Anderson Cancer Center.

[1] Abbreviations: AFM, atomic force microscopy; BPDE, 7r,8t-dihydroxy-9,10t-oxy-7,8,9,10-tetrahydrobenzo[*a*]pyrene diol epoxide; dGua, deoxyguanosine; PCR, polymerase chain reaction; THF, tetrahydrofuran; HEPES/KOH, *N*-(2-hydroxyethyl)piperazine-*N*′-2-ethanesulfonic acid/potassium hydroxide; pGB, pBEND2 plasmid; r_b, fraction of nucleotides modified by carcinogen.

10.1021/tx9902035 CCC: $19.00
Published on Web 04/20/2000

DNA samples were diluted in HM1 buffer [20 mM HEPES/KOH (pH 7.6) and 10 mM magnesium acetate] to a concentration of 2−3 ng/μL. Approximately 8 ng of DNA was adsorbed to a freshly cleaved mica surface (glued to steel disks), allowed to incubate at ambient temperature, then gently washed with Milli-Q water, and dried under a gentle stream of filtered, compressed air. In some cases, the samples were further dried under vacuum. Atomic force microscope (AFM) imaging was performed in tapping mode on a Digital Instruments multimode NanoScope III with a vertical E scanner having a maximal lateral range of approximately 13 μm (*19*, *20*). Standard silicon cantilevers 125 μm in length were used for all tapping in air images. The cantilever oscillation frequency was tuned to 280−320 nm, and samples were scanned at 3−5 lines/s. Images were processed by flattening (using NanoScope software) to remove background slope. All images that are shown were analyzed by tapping in air.

Results and Discussion

DNA molecules that are longer than the normal persistence length of DNA (∼100−150 bp) were modified with BPDE to high levels ($r_b \sim 0.01-0.05$) and visualized by tapping mode atomic force microscopy (AFM). For plasmid-sized, circular DNA (from pGB), there was a dramatic change in the structures seen after modification. Discrete, well-spread-out circles that could be easily measured were seen as the norm with the mock-modified DNA (Figure 1A). The bulk of the circular DNA was observed as relaxed circles. However, molecules modified to a high level with BPDE (from the same plasmid lot as the control) ($r_b \sim 0.05$) tended to clump and exhibit a collapsed appearance (Figure 1B). This made quantitative measurements difficult for the plasmid molecules. Qualitatively, the modified DNA exhibits a "kinkier" appearance than the mock-modified DNA.

Linear DNA molecules 366 bp long were prepared and modified to various levels prior to visualization by AFM. Figure 2 shows representative qualitative images of the effects of the increasing level of modification of BPDE of DNA. Increasing levels of modification led to the appearance of a qualitatively increased level of apparent bends in the DNA. At the highest level of modification ($r_b = 0.036$), toroids were observed (Figure 2D, panels 3 and 5). Golan et al. observed an increase in the extent of toroid formation with increasing polylysine-asialoorosomucoid levels, showing that DNA condenses into toroids under a variety of conditions (*21*). DNA molecules containing high levels of modification were difficult to visualize and difficult to quantify as noted above with the plasmid molecules. One possible reason for this difficulty would be that highly BPDE-modified DNA is refractory to binding to mica. Since mica possesses a slight negative charge, it is possible that the conformational change induced by BPDE on DNA further decreased the DNA affinity for the surface. Hansma and Laney (*22*) showed that divalent cations encouraged adsorption of DNA onto mica. Various buffer conditions were tried, with little success in obtaining enough reproducible images for quantitative analysis of high levels of modification.

The introduction of bends at random into DNA molecules is expected to reduce the persistence length of the DNA, and therefore to lead to more compact molecules with a reduced end-to-end distance. Preparations of linear DNA containing BPDE adducts at intermediate levels of modification ($r_b \sim 0.01-0.02$), or unmodified

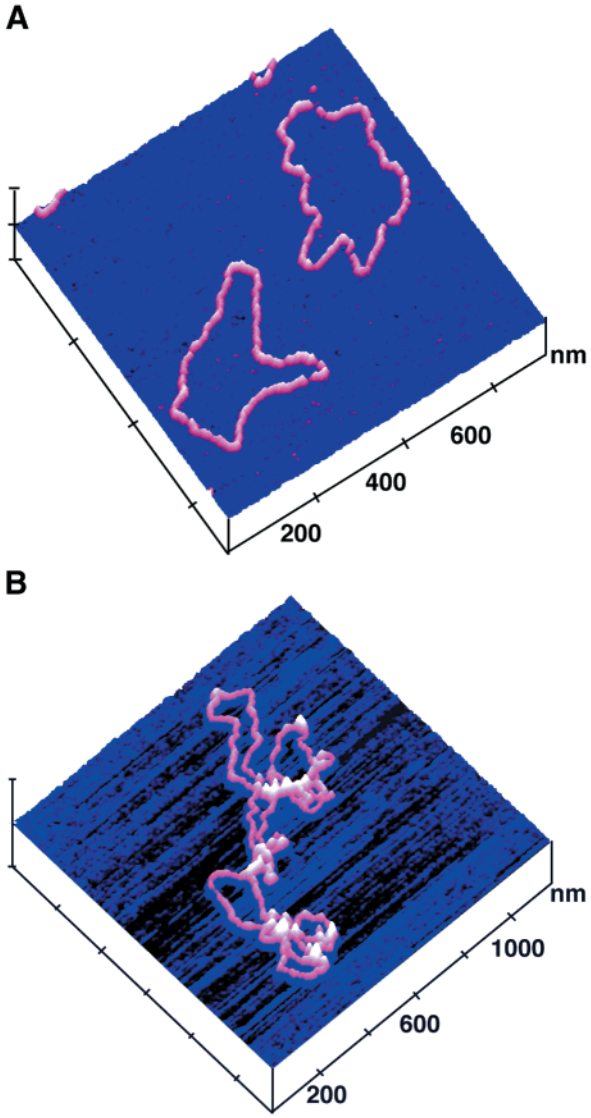

Figure 1. Atomic force microscope image of mock-modified or BPDE-modified plasmid. Representative images are shown of DNA visualized by tapping mode AFM in air: (A) control plasmid and (B) plasmid modified with BPDE ($r_b = 0.051$).

Table 1. Statistical Analysis of Length Parameters of 366 bp DNA[a]

r_b	contour length (nm)	end-to-end distance (nm)	R (end-to-end distance/contour length)
0	118 ± 11	92 ± 17	0.78[b,c] ± 0.12
0.011	124 ± 8	90 ± 20	0.73[b] ± 0.16
0.020	117 ± 13	69 ± 22	0.59[c] ± 0.17

[a] AFM images of either mock-modified or BPDE-modified DNA were obtained. In each case, contour lengths and end-to-end distances were measured for at least 100 molecules that could unequivocally be traced. [b] Difference between means statistically significant as determined by an unpaired t test ($P < 0.01$). [c] Difference between means statistically significant by as determined an unpaired t test ($P < 0.0001$).

DNA, were visualized by AFM. The digital images of at least 100 molecules in each preparation were analyzed for contour length and end-to-end distance. Frequency distributions of these data are shown in Figure 3, and average values are collected in Table 1. Measurements of the control and BPDE-modified DNA populations indicated no significant change in the contour length at the highest level of modification ($r_b = 0.02$, Figure 3A and Table 1). However, the distribution of end-to-end

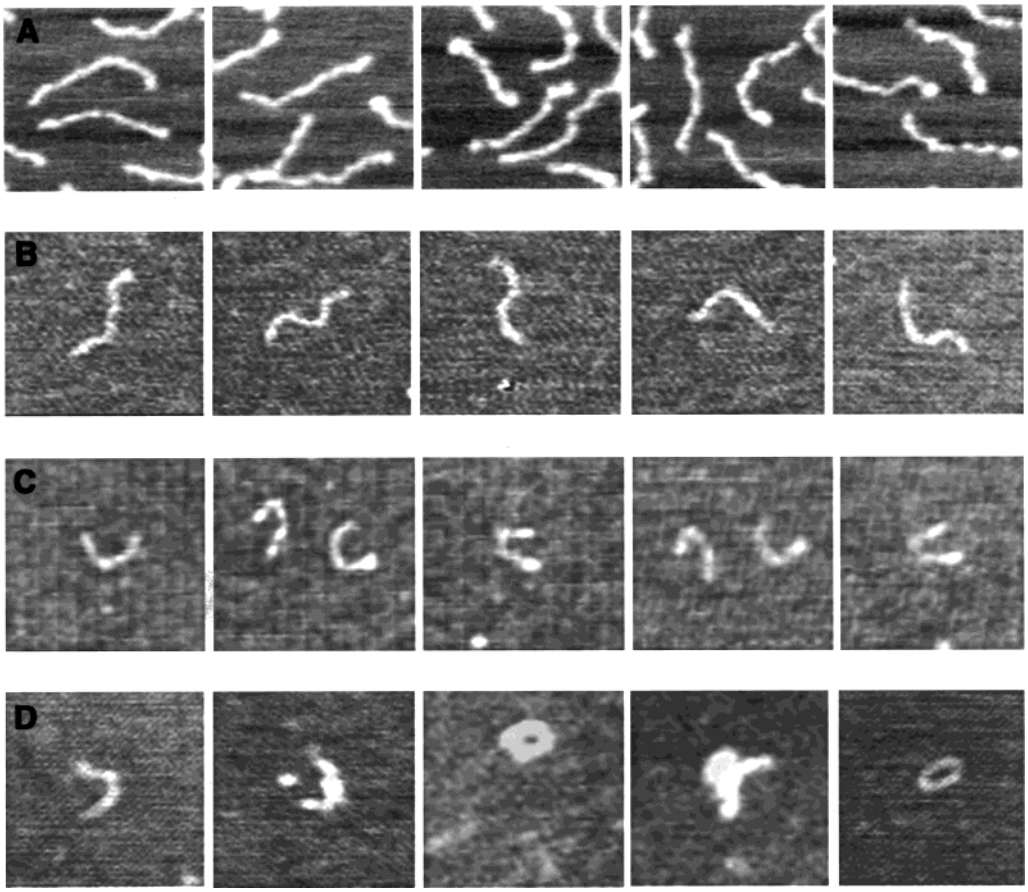

Figure 2. Atomic force microscopy of BPDE-modified linear DNA containing increasing concentrations of adducts. Preparations of 366 bp long, linear DNA were modified with BPDE to attain an r_b of (A) 0.00, (B) 0.011, (C) 0.025, and (D) 0.036, and then visualized by tapping mode AFM. Five representative images of each preparation are shown.

distances was progressively skewed toward smaller values with an increasing level of modification (Figure 3B). When $r_b = 0.01$ (shaded bars), there was an increase in the fraction of molecules with very short (<60 nm) end-to-end distances, whereas when $r_b = 0.02$ (solid bars), the entire distribution had shifted toward lower values. Nonparametric rank tests (Mann Whitney) indicated a significant change in the distribution when $r_b = 0.02$. The average ratio of end-to-end distance to contour length for molecules with an r_b of either 0.01 or 0.02 was significantly smaller than with control DNA (Table 1). When $r_b = 0.02$, this ratio had decreased by about 25%. This is direct evidence that BPDE−DNA adducts induce measurable bends in DNA molecules.

To begin to relate the AFM images of BPDE-modified DNA to adduct-induced bends, we constructed theoretical distributions of the ratio of end-to-end distance to contour length using a two-dimensional random walk model to simulate the path of individual DNA molecules in the AFM images. Simulated molecules were generated by Monte Carlo methods using a 366-step random walk (1 step for each base pair). At each step, the direction of the path of the DNA was allowed to deviate from the previous direction by an angle, θ, drawn at random from a normal distribution with a mean μ and a standard deviation σ. Clockwise and counterclockwise changes of direction were assigned randomly with equal probability. At the end of the walk, the ratio of the end-to-end distance to the contour length (R) was determined. To model unmodified DNA, μ was set to zero and σ was varied until the distribution of R values was similar to the measured distribution. The quartile distribution of R values shown in Figure 4 (left panel, white bars) for 900 random walks with a σ of 5.7° is comparable to the distribution of R values determined experimentally for unmodified DNA (solid bars). To model BPDE-modified DNA, we randomly assigned each step of the walk as either a normal or an adduct-containing step with relative probabilities such that the overall level of modification r_b was 0.01 (center panel) or 0.02 (right panel). For adduct-containing steps, we used a distribution of θ with a non-zero μ, but the same σ as for normal steps and again assigned clockwise and counterclockwise changes of direction with equal probability. A given trial value of μ was used to conduct 900 random walks, and the quartile distribution of the data set was compared to experimental data with an r_b of 0.01 or 0.02. With a μ of 30°, the theoretical distributions were similar to the experimental distributions for modified DNA (Figure 4), although the theoretical distributions exhibited more dispersion.

We cannot assign a 1:1 correspondence between the theoretical value for μ and the average bend angle induced by the BPDE adduct because we do not know the detailed mechanism by which the three-dimensional DNA molecules assume a particular two-dimensional path on the mica surface. However, the constraints introduced by this process are likely to tend to minimize the overall angular distribution, especially in cases where two ends of a molecule attach to the surface indepen-

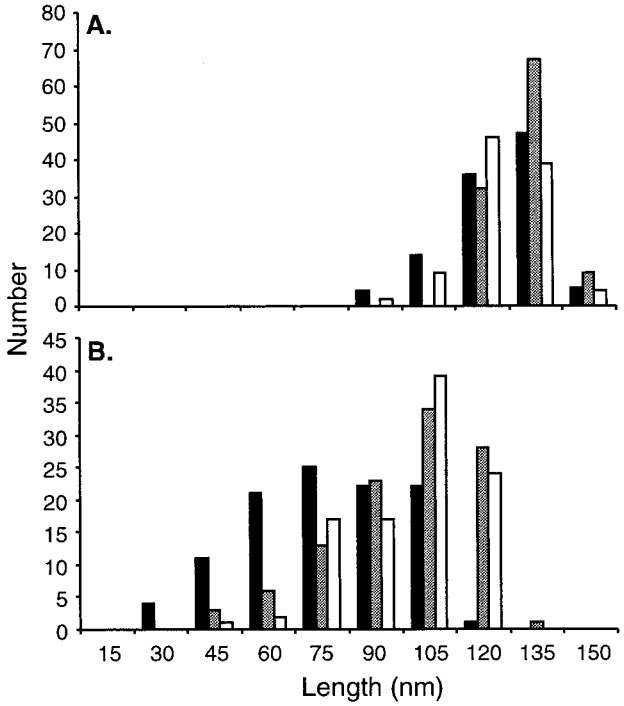

Figure 3. Frequency distributions of contour lengths and end-to-end distances. Tapping mode AFM images of mock-modified (white bars) or BPDE-modified [$r_b = 0.011$ (shaded bars), $r_b = 0.02$ (black bars)] linear DNA were analyzed with Oncor Image software. At least 100 isolated molecules in each preparation without apparent overlaps were traced, and the contour length and end-to-end length were measured. In each image, all molecules that could be unequivocally traced from end to end were included in the data set. Frequency distributions for (A) contour lengths and (B) end-to-end distances are shown. Numbers along the abcissa indicate the upper limit of each frequency interval.

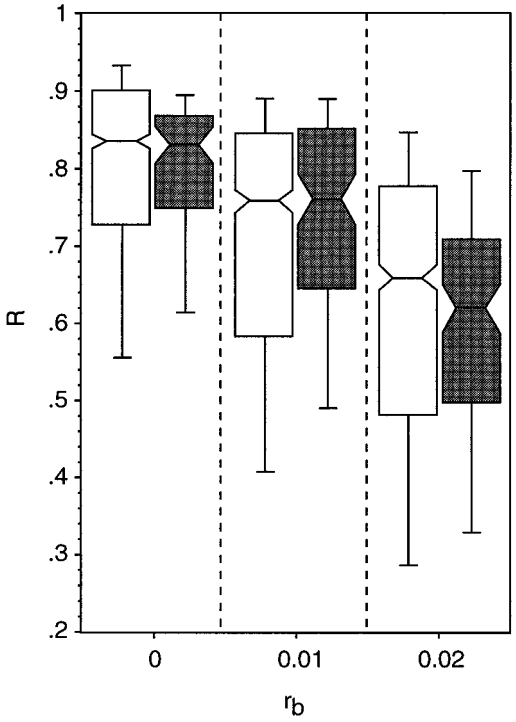

Figure 4. Comparison of experimental with theoretical distributions using a random walk model. The experimental data sets from Table 1 are shown as box plots (shaded bars), where the boxes indicate the middle two quartiles of the distribution. Using the parameters discussed in the text, 900 random walks were calculated for each of three levels of modification to give the model data sets (white bars).

dently. Therefore, our data suggest 30° as a minimum estimate of the average bend angle induced by BPDE adducts in double-stranded DNA.

Previous electrophoretic studies of short fragments of DNA randomly modified with BPDE to levels similar to those used here provided the first suggestion that BPDE−DNA adducts bend DNA (*13*), although no estimation of the magnitude of this effect was made. More recent studies with defined sequence oligonucleotides bearing a single BPDE adduct have provided both electrophoretic evidence for bending and evidence based on the ease of circularization to produce minicircles (*14*−*17*). For the major adduct derived from racemic BPDE, the average magnitude of the induced bend in the sequence context TGT was estimated to be 40° (*16*); in the CGC context, the magnitude of the effect appeared to be even larger (*17*). Thus, our rough estimation, averaged over many different sequence contexts, is consistent with those made in defined contexts. It should be noted that previously measured changes in electrophoretic mobility could also be partially explained by an adduct-induced increase in contour length. Although decreases in contour length due to formation of platinum−DNA adducts have been reported using AFM (*23*), no consistent changes in length due to BPDE adducts were detected in the studies presented here. Tapping mode AFM appears to be an excellent tool for monitoring the overall effects of DNA damage on conformation. It will be of interest to attempt to measure the effects of single, defined adducts using this technique.

Acknowledgment. This work was supported by Grant CA35581 from the National Cancer Institute (M.C.M.), by Grants MCB 9604566 (L.I.P.) and DMR 96-32716 (B.L.S.) from the National Science Foundation, by Grant DAAHO4-96-1-0443 from the Army Research Office, MURI Program (B.L.S.), and by an NIEHS Center Grant (ES07784). We thank Dennis Johnston for statistical advice and Rebecca Deen for manuscript preparation.

References

(1) Jeffrey, A. M., Weinstein, I. B., Jennette, K. W., Grzeskowiak, K., Nakanishi, K., Harvey, R. G., Autrup, H., and Harris, C. (1977) Structures of benzo[*a*]pyrene−nucleic acid adducts formed in human and bovine bronchial explants. *Nature* **269**, 348−350.

(2) Straub, K. M., Meehan, T., Burlingame, A. L., and Calvin, M. (1977) Identification of the major adducts formed by reaction of benzo[*a*]pyrene diol epoxide with DNA in vitro. *Proc. Natl. Acad. Sci. U.S.A.* **74**, 5285−5289.

(3) Cheng, S. C., Hilton, B. D., Roman, J. M., and Dipple, A. (1989) DNA adducts from carcinogenic and noncarcinogenic enantiomers of benzo[*a*]pyrene dihydrodiol epoxide. *Chem. Res. Toxicol.* **2**, 334−340.

(4) Moore, P., and Strauss, B. S. (1979) Sites of inhibition of in vitro DNA synthesis in carcinogen- and UV-treated phi X174 DNA. *Nature* **278**, 664−666.

(5) MacLeod, M., Powell, K., and Tran, N. (1995) Binding of the transcription factor, Sp1, to non-target sites in DNA modified by benzo[*a*]pyrene diol epoxide. *Carcinogenesis* **16**, 975−983.

(6) Yang, L. L., Maher, V. M., and McCormick, J. J. (1982) Relationship between excision repair and the cytotoxic and mutagenic effect of the "anti" 7,8-diol-9,10-epoxide of benzo[*a*]pyrene in human cells. *Mutat. Res.* **94**, 435−447.

(7) Brookes, P., and Osborne, M. R. (1982) Mutation in mammalian cells by stereoisomers of anti-benzo[*a*]pyrene diol epoxide in relation to the extent and nature of the DNA reaction products. *Carcinogenesis* **3**, 1223−1226.

(8) Slaga, T. J., Bracken, W. J., Gleason, G., Levin, W., Yagi, H., Jerina, D. M., and Conney, A. H. (1979) Marked differences in the skin tumor-initiating activities of the optical enantiomers of

the diastereomeric benzo[*a*]pyrene 7,8-diol-9,10-epoxides. *Cancer Res.* **39**, 67−71.
(9) MacLeod, M. C., Adair, G., Daylong, A., Lew, L., and Humphrey, R. M. (1991) Low absolute mutagenic efficiency but high cytotoxicity of a non-bay region diol epoxide derived from benzo[*a*]pyrene. *Mutat. Res.* **261**, 281−293.
(10) MacLeod, M. C., Daylong, A., Adair, G., and Humphrey, R. M. (1991) Differences in the rate of DNA adduct removal and the efficiency of mutagenesis for two benzo[*a*]pyrene diol epoxides in CHO cells. *Mutat. Res.* **261**, 267−279.
(11) Rodriguez, H., and Loechler, E. L. (1993) Mutagenesis by the (+)-anti-diol epoxide of benzo[*a*]pyrene: what controls mutagenic specificity? *Biochemistry* **32**, 1759−1769.
(12) Jelinsky, S. A., Liu, T., Geacintov, N. E., and Loechler, E. L. (1995) The major, N2-Gua adduct of the (+)-anti-benzo[*a*]pyrene diol epoxide is capable of inducing G → A and G → C, in addition to G → T, mutations. *Biochemistry* **34**, 13545−13553.
(13) Hogan, M. E., Dattagupta, N., and Whitlock, J. P., Jr. (1981) Carcinogen-induced alteration of DNA structure. *J. Biol. Chem.* **256**, 4504−4513.
(14) Xu, R., Mao, B., Xu, J., Li, B., Birke, S., Swenberg, C. E., and Geacintov, N. E. (1995) Stereochemistry-dependent bending in oligonucleotide duplexes induced by site-specific covalent benzo[*a*]pyrene diol epoxide-guanine lesions. *Nucleic Acids Res.* **23**, 2314−2319.
(15) Liu, T., Xu, J., Tsao, H., Li, B., Xu, R., Yang, C., Amin, S., Moriya, M., and Geacintov, N. E. (1996) Base sequence-dependent bends in site-specific benzo[*a*]pyrene diol epoxide-modified oligonucleotide duplexes. *Chem. Res. Toxicol.* **9**, 255−261.
(16) Xu, R., Mao, B., Amin, S., and Geacintov, N. E. (1998) Bending and circularization of site-specific and stereoisomeric carcinogen-DNA adducts. *Biochemistry* **37**, 769−778.
(17) Tsao, H., Mao, B., Zhuang, P., Xu, R., Amin, S., and Geacintov, N. E. (1998) Sequence dependence and characteristics of bends induced by site-specific polynuclear aromatic carcinogen-deoxyguanosine lesions in oligonucleotides. *Biochemistry* **37**, 4993−5000.
(18) Kerppola, T. K., and Curran, T. (1991) DNA bending by Fos and Jun: the flexible hinge model. *Science* **254**, 1210−1214.
(19) Binnig, G., Quate, C. F., and Gerber, C. (1986) The Atomic Force Microscope. *Phys. Rev. Lett.* **56**, 930−933.
(20) Hansma, P. K., Cleveland, J. P., Radmacher, M., Walters, D. A., Hillner, P. E., Bezanilla, M., Fritz, M., Vie, D., Hansma, H. G., Prater, C. B., Massie, J., Fukunaga, L., Gurley, J., and Elings, V. (1994) Tapping mode atomic force microscopy in liquids. *Appl. Phys. Lett.* **64**, 1738−1740.
(21) Golan, R., Pietrasanta, L. I., Hsieh, W., and Hansma, H. G. (1999) DNA toroids: stages in condensation. *Biochemistry* **38**, 14069−14076.
(22) Hansma, H. G., and Laney, D. E. (1996) DNA binding to mica correlates with cationic radius: assay by atomic force microscopy. *Biophys. J.* **70**, 1933−1939.
(23) Onoa, G. B., Cervantes, G., Moreno, V., and Prieto, M. J. (1998) Study of the interaction of DNA with cisplatin and other Pd(II) and Pt(II) complexes by atomic force microscopy. *Nucleic Acids Res.* **26**, 1473−1480.

TX9902035